Int. Journal of Refractory Metals and Hard Materials 36 (2013) 111–115

Contents lists available at SciVerse ScienceDirect

Int. Journal of Refractory Metals and Hard Materials

journal homepage: www.elsevier.com/locate/IJRMHM

Comparison of metastable phases induced by heat treatment of unmilled and milled cobalt powders

A.S. Bolokang [a,*], M.J. Phasha [b,*], S. Bhero [a]

[a] Department of Engineering Metallurgy, University of Johannesburg, P.O. Box 17011, Doornfontein 2028, South Africa
[b] Council for Scientific and Industrial Research (CSIR), Materials Science and Manufacturing, Meiring Naude, Brummeria, P.O. Box 395, Pretoria 0001, South Africa

ARTICLE INFO

Article history:
Received 22 March 2012
Accepted 3 August 2012

Keywords:
Cobalt
Water quenching
Metastable phases
Mechanical milling
XRD

ABSTRACT

The sintered and water quenched compact samples were prepared from unmilled and milled Co powders. Characterisation was performed by differential scanning calorimetry, scanning electron microscopy and X-ray diffraction techniques. Several metastable phases were obtained upon sintering and quenching. However, more metastable phases were induced on quenching the milled–sintered samples due to introduction of large number of defects in addition to those induced by milling. Micro hardness values for unmilled sintered samples were the lowest while those of 30 h milled-sintered samples were the highest. The current study reveals that the two FCC metastable phases obtained by quenching unmilled powder were similar to those found in milled–sintered samples.

1. Introduction

Rapid cooling of pure or metallic alloys from elevated temperature is one of the oldest traditional methods to induce phases with novel mechanical properties. Due to fast cooling, material does not have enough time to obey its normal thermodynamic transformation route. This process is therefore said to be non-equilibrium in nature. The type of rapid cooling methods to be used depends on the end application of the product. For example, Ti–Ni atomised powder is produced by fast cooling from liquid metal under inert gas [1–3]. As a result, the crystallographic relation between the austenite (B2) and martensitic (B19′) phases, which resembles shape memory effect, can be induced. It implies that the high temperature phase (B2) is deformed to yield the martensite at low temperature due to fast cooling. Furthermore, magnetron sputtering deposition of Ni–W thin films yielded metastable phases such as hexagonal-close-packed (HCP) and face-centered-cubic (FCC) eta (η) [4]. The Co–W alloy produced by deposition results in good magnetic, corrosion, wear resistance and high hardness [5–7]. However, despite the fact that water-quenching (WQ) is one of the oldest and versatile processes used in the field of metallurgy in order to obtain good mechanical properties in different alloys, reports on WQ of pure metals are scarce. Zhao et al. [8] have reported $\beta \rightarrow \alpha'$ martensitic phase transformation in pure titanium which showed the unique microstructure as a result of quenching. It has been shown that FCC nickel could transform to a mixture of HCP and FCC phases by water quenching [9]. Similarly, water-quenching of body-centered-cubic (BCC) iron revealed a mixture of HCP and FCC phases [10]. Cobalt also has been reported to yield HCP/FCC bi-phasic mixture upon quenching [11,12]. Accordingly, the existence FCC phase in Co was obtained when grains are fine while HCP appears on coarse grains [12]. It thus follows that the three ferromagnetic elements (Ni, Fe, and Co) tend to favour a bi-phasic FCC/HCP mixture when quenched. Although metastable phases are often obtained by heat treatment and rapid cooling, their formations are also possible via low temperature mechanical deformation processes such as cold pressing (CP) and mechanical milling (MM). The FCC → HCP phase transformation in Co powder induced by CP has been reported previously [13,14]. In addition, an intermetallic phase formation is considered possible through repeated cold pressing of Sn and Te elemental mixture [15]. Alternatively, MM is a versatile powder deformation processing technique that is well known to induce metastable phases in elemental powders [14,16–23]. This easy and cost-effective process introduces structural defects, stacking faults as well as dislocation in metallic powders. The presence of metastable phases obtained on milled Co after annealing was recently published [14,24]. These findings raised further curiosity on the effect of non-equilibrium processing techniques on elemental Co powder. So far, there is a lack of information in literature on metastable phases of Co induced by water-quenching the mechanically milled powders. Hence, the purpose of the current investigation is to compare the metastable phases of unmilled and milled Co, after sintering and water-quenching.

2. Experimental work

Commercial Co powder of 99.8% was milled under argon atmosphere at milling speed of 650 rpm for 30 h. Milling was performed in the stainless steel milling medium consisting of 5 mm diameter balls and vial at ball-to-powder ratio of 20:1. Milling vial was equipped

* Corresponding authors. Tel.: +27 12 841 3196; fax: +27 12 841 3378.
E-mail addresses: amogelangblkng6@gmail.com (A.S. Bolokang), mphasha@csir.co.za (M.J. Phasha).

0263-4368/$ – see front matter © 2012 Elsevier Ltd. All rights reserved.
http://dx.doi.org/10.1016/j.ijrmhm.2012.08.001

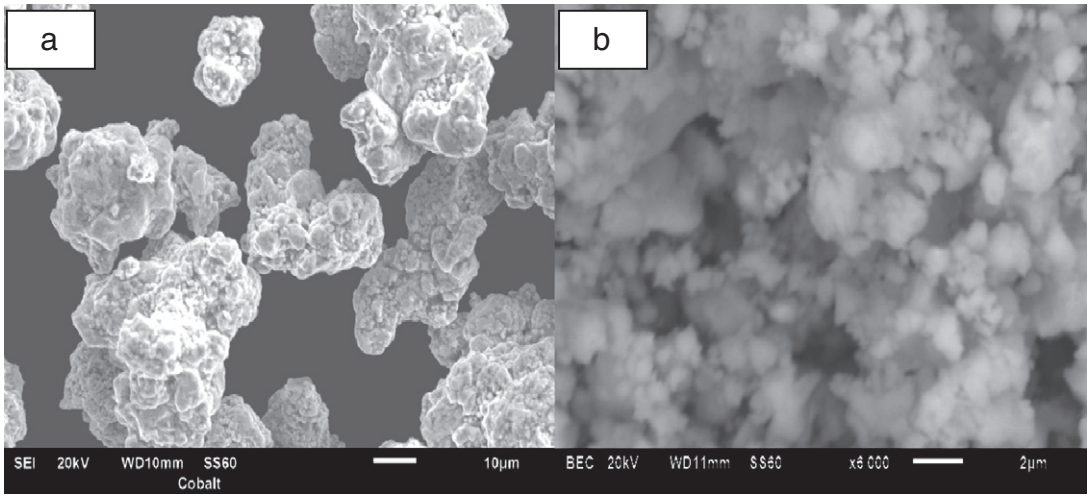

Fig. 1. SEM images of (a) unmilled, (b) 30-h milled cobalt powders.

with cooling system (water jacket) to avoid heating during milling. A small powder sample was used for crystal structure analysis and morphology. Unmilled and milled powders were cold pressed at a pressure of 20 MPa to form cylindrical compacts of 17 mm diameter. These compacts were sintered in a tube furnace at temperature of 1200 °C for 1 hour (h) followed by furnace cooling in some while others were quenched in water at room temperature. The microstructural analysis was carried out on mounted and polished cross-sections of the sintered/quenched samples using LEO 1525 field-emission scanning electron microscope (FE-SEM) coupled with a Robinson Backscatter Electron Detector (RBSD) and an Oxford Link Pentafet energy dispersive X-ray spectroscopy (EDX) detector. Phase evolution was traced with a Phillips PW 1830 X-ray diffraction (XRD) machine fitted with Cu Kα radiation, and 0.02 step size scanned from 20° to 90° (2θ). Thermal analysis was carried out using DSC and TG incorporated in NETZSCH STA. Milled Co powder sample was heated up to 1200 °C with Al_2O_3 as a baseline. A heating rate of 20 °C min^{-1} under argon gas at 20 mL/L standard flow rate was used. The macro-hardness measurements were carried out using FV-700 Vickers hardness tester with 2 kg load. The densities as well as the crystallite sizes of sintered samples were determined using Archimedes principle and Scherrer equation [18], respectively.

3. Results and discussion

Fig. 1(a) and (b) shows the SEM pictures of unmilled and 30 h mechanically milled Co powders, respectively. From these images, it is clear that the irregular particles of unmilled Co particles got refined with smooth surfaces as in Fig. 1(b). Furthermore, these fine particles seem to have agglomerated. To validate the size reduction, the measured particle sizes of unmilled and milled powders are presented in Table 1. Unmilled particle diameter for cumulative 10 (D_{10}), 50 (D_{50}) and 90 (D_{90}) wt.% are 19, 32 and 52 μm respectively, while for milled are 2, 7 and 19 μm, respectively.

The phase transformation induced by MM of Co powder was recently discussed in detail by the same authors [14]. XRD patterns of unmilled, sintered and water quenched samples are shown in Fig. 2(a), (b) and (c), respectively. The as-received powder is composed of only HCP

Table 1
Particle size distribution of unmilled and MM Co powders.

Powder (μm)	D_{10}	D_{50}	D_{90}
Unmilled	19	32	52
30 h milled	2	7	19

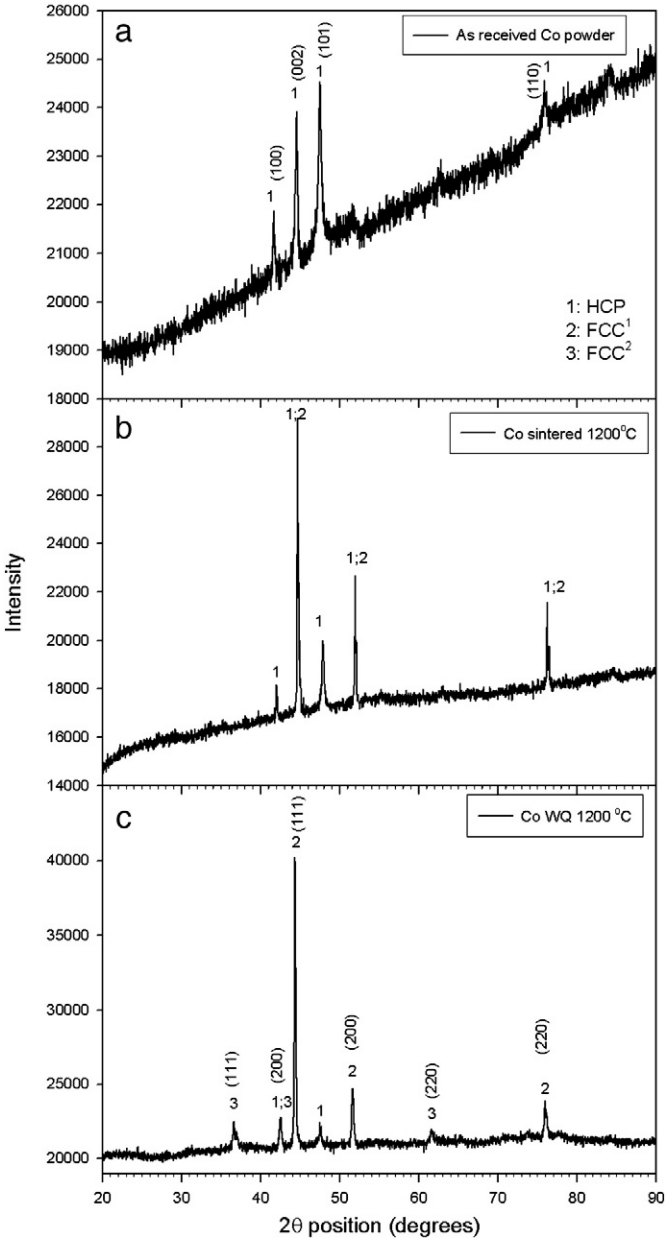

Fig. 2. XRD patterns of Co (a) unmilled, (b) sintered at 1200 °C and (c) WQ from 1200 °C.

Table 2
XRD data for Co powder treated under various conditions.

Condition	Phases	Lattice parameter (Å)		
		a	b	c
Unmilled powder	HCP	2.51	–	4.08
30 h milled powder	FCC	3.80 [14]	–	–
Unmilled–sintered at 1200 °C	HCP	2.51	–	4.07
	FCC^1	3.52	–	–
Unmilled–sintered and WQ at 1200 °C	FCC^1	3.54	–	–
	FCC^2	4.25	–	–
	HCP	2.50		4.06
30 h milled–sintered at 1200 °C	FCC^1	3.55	–	–
	FCC^2	4.21	–	–
30 h milled–sintered and WQ at 1200 °C	MCL	5.74	5.03 (β = 114°)	5.40
	CUB	8.06	–	–
	RHL	4.96	–	13.59
	FCC^2	4.16	–	–

phase with weak signals of FCC phase. However, due to incomplete reverse martensitic transformation, the presence of the high temperature FCC phase (denoted here as FCC^1) is evident upon sintering. Furthermore, when the sintered compacts were water-quenched, two types of FCC phases (FCC^1 and FCC^2) and small trace of HCP phase were detected by the XRD.

The corresponding lattice parameters of HCP and FCC phases are presented in Table 2. The lattice parameters of these FCC phases are 3.54 and 4.25 Å for FCC^1 and FCC^2, respectively. The FCC^2 phase is associated with B1-type CoO phase. These results showing co-existence of two different types of FCC phases are similar to those obtained previously for water-quenched nickel [9].

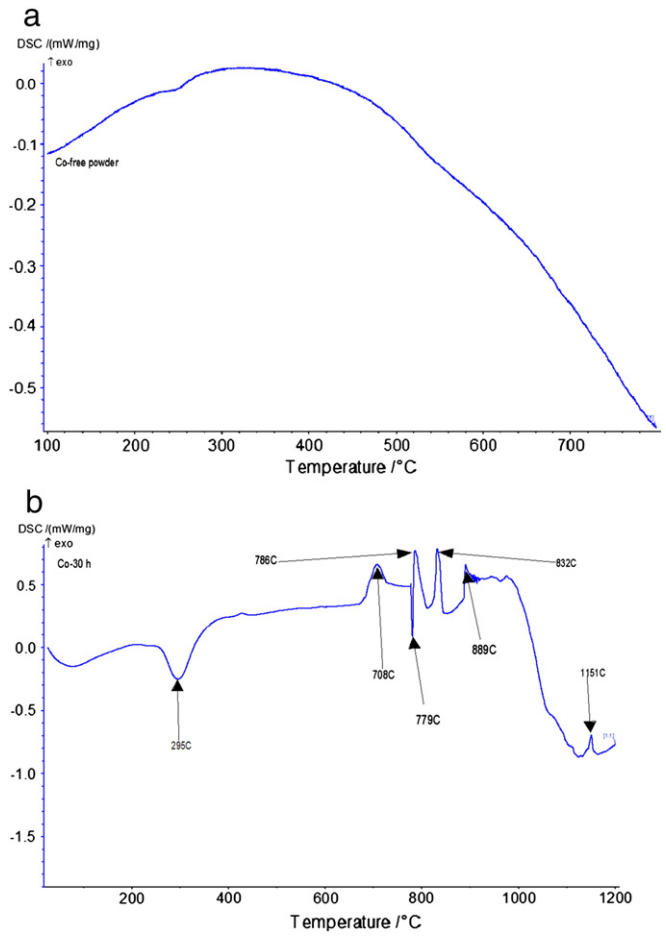

Fig. 3. DSC curve of (a) unmilled and (b) 30 h milled Co powders.

Fig. 3(a) and (b) shows thermal analysis by DSC for temperature up to 800 °C and 1200 °C for unmilled and 30 h milled Co powder. The DSC curve of unmilled powder was discussed in detail in Ref. [24] and it is only included here for comparison purposes. From the DSC curve of 30 h milled powder, endothermic and exothermic peaks are observed at 295 and 708 °C, respectively. The former is commonly associated with lattice recovery or strain relief in milled powders while the latter is attributed to lattice reordering to usual FCC phase with lattice parameter of 3.54 Å. Furthermore, there is a sharp endothermic peak at 779 °C followed by three exothermic peaks at 786, 832, 859 and 1151 °C, respectively. These multiple peaks are an indication of inhomogeneity in milled particles, thus transforming and/or oxidizing at different temperatures. To average the phase representation of these multiple peaks, the 30 h milled Co powder was sintered well above these temperatures and water quenched from 1200 °C.

In Fig. 4, the XRD patterns of milled–sintered and milled–sintered–water-quenched samples are shown together with that of unmilled powder for comparison. The two FCC phases similar to those observed on

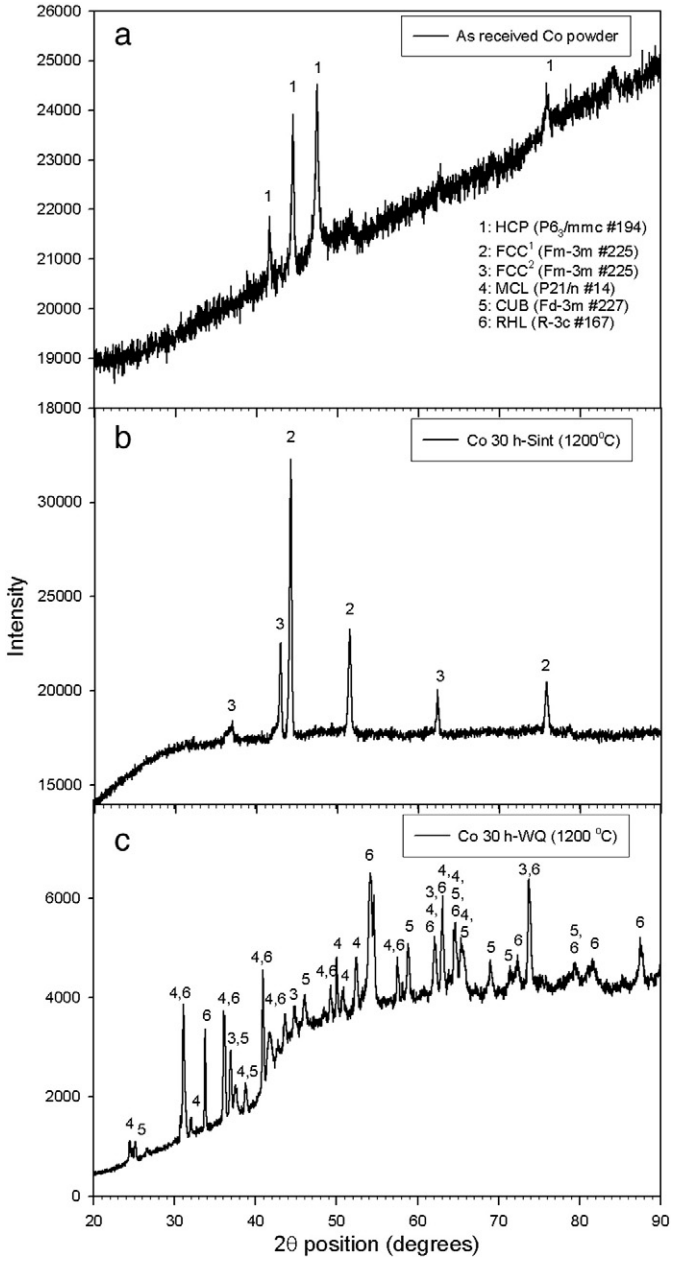

Fig. 4. XRD patterns of (a) unmilled, (b) 30 h milled–sintered and (c) 30 h milled–sintered–WQ at 1200 °C.

Table 3
Calculated densities and crystallite sizes estimated using Scherrer equation of the as-sintered Co samples.

Sample	Density (g/cm^3)	% Theoretical density	D (nm)
Unmilled–sintered	7.3	81	224 (FCC^1) 216 (HCP)
Unmilled–sintered and quenched	7.4	83	168 (FCC^1) 95 (FCC^2) 85 (HCP)
30 h milled and sintered	8.2	92	84 (FCC^1) 95 (FCC^2)
30 h milled–sintered and quenched	7.8	88	129 (MCL) 129 (CUB) 108 (RHL) 55 (FCC^2)

quenching the unmilled Co were evident upon sintering the milled samples at 1200 °C, as shown in Fig. 4(b). The corresponding lattice parameters for these phases are 3.55 and 4.21 Å, with the lattice parameter of latter being attributed to oxygen deficient CoO_{1-x} phase. These results seem to imply that the stresses induced by WQ unmilled Co have similar effect to those caused by sintering milled powder. However, the mechanical properties may vary due to difference in crystallite sizes and densities of the materials, as will be shown in Fig. 6 and Table 3. Fig. 4(c) shows the XRD pattern for samples milled–sintered and quenched at 1200 °C. An erratic type of pattern has emerged, probably due to high disordering induced by the combination effect of milling and quenching. However, the complex nature for the resulting XRD pattern posed a challenge to accurately identify present phases. Nevertheless, about four slightly overlapping major phases were identified as monoclinic (MCL), cubic (CUB), rhombohedral (RHL) and FCC^2 with closest space groups shown in parentheses. The corresponding approximated lattice parameters are also listed in Table 2. So far, the presence of these phases is ascribed to abrupt forced transformation due to additional structural defects introduced by WQ on addition to MM induced disorder, which occurs mainly due to the presence of oxygen deficient compound such as CoO_{1-x}. Although the scientific reasons behind the formation of these phases are uncertain at this point, a similar correlation between RHL and FCC cubic phases could exist, as was observed previously on sintering ball milling induced FCC titanium powder [18]. As indicated by equal crystallite size, the MCL phase could either be the intermediate phase between RHL and CUB phases or martensitic metastable phase.

The SEM images of sintered and quenched samples are presented in Fig. 5(a)–(d). Generally, the microstructures of quenched samples (b and d) appear different when compared to those of only sintered samples (a and c). Furthermore, Fig. 5(c) and (d) evidently shows the existence of multiple phase microstructures, which validates the XRD results.

The corresponding densities, crystallite sizes of present phases and average Vickers hardness values of sintered and water-quenched samples are presented in Table 3 and Fig. 6. It is evident that the increased hardness upon water-quenching the unmilled–sintered samples is due to grain refinement as indicated by smaller crystallite size in Table 3. However, water-quenching the 30 h milled–sintered samples yielded larger crystallite size, and consequently lower hardness than the as-sintered samples. This behaviour further indicates the significant role of grain size in the mechanical properties of heat treated unmilled and milled powders.

4. Conclusions

Metastable phases were obtained upon sintering and quenching the unmilled and milled Co samples. However, more metastable phases were induced on quenching the milled–sintered samples due to introduction of large number of defects. The created dislocation and vacancies provided the nucleation sites for metastable phases. The current study

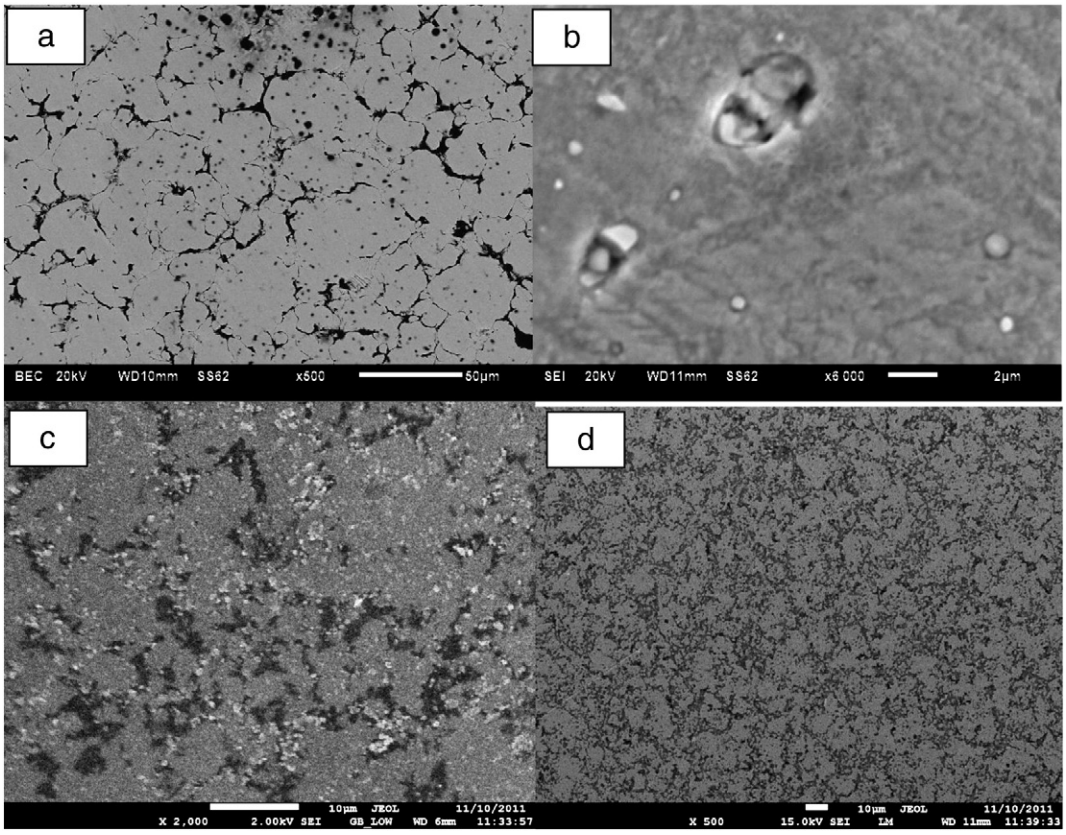

Fig. 5. SEM micrographs of Co (a) unmilled–sintered, (b) unmilled–sintered–water-quenched, (c) 30 h milled–sintered and (d) 30 h milled–sintered–water-quenched.

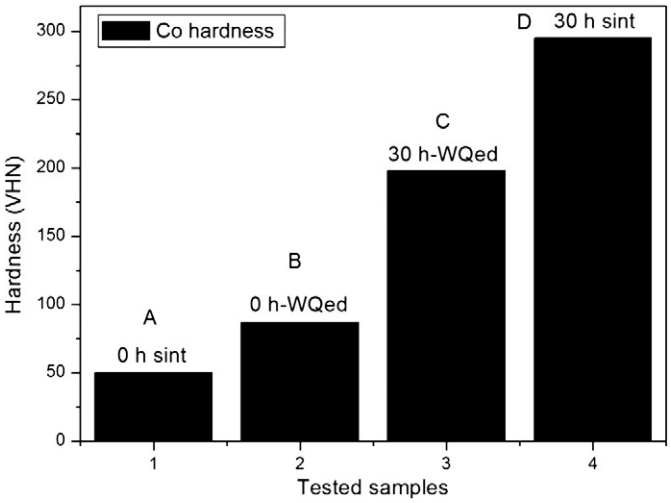

Fig. 6. Vickers hardness of sintered and water-quenched samples.

reveals that similar FCC metastable phases were obtained from unmilled–water-quenched samples as well as milled–sintered samples. Water-quenching the 30 h milled–sintered samples yielded larger crystallite size, and consequently lower hardness than the as-sintered counterparts. This behaviour further indicates the significant role of grain size in the mechanical properties of heat treated unmilled and milled powders.

Acknowledgement

This work was supported by the Department of Engineering Metallurgy at the University of Johannesburg.

References

[1] Porter GA, Liaw PK, Tiegs TN, Wu KH. Particle size reduction of NiTi shape-memory alloy powders. Scr Mater 2000;43:1111-7.
[2] Kim Y-W, Jeon K-S, Yun Y-M, Nam T-H. Microstructure and shape memory characteristics of gas-atomized TiNi powders. Phys Scr 2010;T139:1-4.
[3] Yamamoto T, Kato H, Murakami Y, Kimura H, Inoue A. Martensitic transformation and microstructure of Ti-rich Ti–Ni gas-atomized powders. Acta Mater 2008;56:5927-37.
[4] Borgia C, Scharowsky T, Furrer A, Solenthaler C, Spolenak R. A combinational study on the influence of elemental composition and heat treatment on the phase composition, microstructure and mechanical properties of Ni–W alloy thin films. Acta Mater 2011;59:386-99.
[5] Yang B, Qin G, Pei W, Ren Y, Xiao N, Zhao X. Abnormal saturation magnetization dependency on W content for Co–W thin films. Acta Metall Sin 2010;23:8–12.
[6] Grabchikov SS, Yaskovich AM. Effect of the structure of amorphous electrodeposited Ni–W and Ni–Co–W alloys on their crystallization. Russ Metall 2006;2006:56-60.
[7] Sheikholeslam MA, Enayati MH, Raessi K. Characterization of nanocrystalline and amorphous cobalt–phosphorus electrodeposits. Mater Lett 2008;62:3629-31.
[8] Zhao W, Zhang W, Guo J, Wang B, Guo J, Lu K. Microstructure evolution and tensile properties of pure Ti subjected to rapidly heating and quenching. J Mater Sci Technol 2006;22:190-4.
[9] Bolokang AS, Phasha MJ. Novel synthesis of metastable HCP Ni by water quenching. Mater Lett 2011;65:59-60.
[10] Belonoshko AB, Derlet PM, Mikhaylushkin AS, Simak SI, Hellman O, Burakovsky L, et al. Quenching of bcc-Fe from high to room temperature at high-pressure conditions: a molecular dynamics simulations. New J Phys 2009;11:1-8.
[11] Owen EA, Madoc Jones D. Effect of grain size on the crystal structure of cobalt. Proc Phys Soc B 1954;67:456-66.
[12] Kajiwara S, Ohno S, Honma K, Uda M. A new crystal structure of pure cobalt in ultrafine particles. Philos Mag Lett 1987;55:215-9.
[13] Karin A, Bonefačić A, Dužević D. Phase transformation in pressed cobalt powder. J Phys F Met Phys 1984;14:2781-6.
[14] Bolokang AS, Phasha MJ, Motaung DE, Bhero S. Effect of mechanical milling and cold pressing on Co powder. J Metall 2012:1-7 [Article ID 290873].
[15] De la Torre SD, Ishihara KN, Shingu PH. Synthesis of SnTe by repeated cold-pressing. Mater Sci Eng A 1999;266:37-43.
[16] Manna I, Chattopadhyay PP, Nanadi P, Banhart F, Fecht HJ. Formation of face-centered-cubic titanium by mechanical attrition. J Appl Phys 2003;93:1520-4.
[17] Chattopadhyay PP, Pabi SK, Manna I. A metastable allotropic transformation in Nb induced by planetary ball milling. Mater Sci Eng A 2001;304–306:424-8.
[18] Phasha MJ, Bolokang AS, Ngoepe PE. Solid-state transformation in nanocrystalline Ti induced by ball milling. Mater Lett 2010;64:1215-8.
[19] Chatterjee P, Sen Gupta SP. An X-ray diffraction study of nanocrystalline titanium prepared by high-energy vibrational ball milling. Appl Surf Sci 2001;182:372-6.
[20] Huang JY, Wu YK, Ye HQ, Lu K. Allotropic transformation of cobalt induced by ball milling. Nanostruct Mater 1995;6:723-6.
[21] Sort J, Nogues J, Surinach S, Baro MD. Microstructural aspects of the hcp–fcc allotropic phase transformation induced by ball milling. Philos Mag 2003;83:439-55.
[22] Sort J, Nogues J, Surinach S, Munoz JS, Baro MD. Correlation between stacking fault formation, allotropic phase transformations and magnetic properties of ball-milled cobalt. Mater Sci Eng A 2004;375–377:869-73.
[23] Delogu F. Kinetics of allotropic phase transformation in cobalt powders undergoing mechanical processing. Scr Mater 2008;58:126-9.
[24] Bolokang AS, Phasha MJ, Camagu ST, Motaung DE, Bhero S. Effect of thermal treatment on mechanically milled cobalt powder. Int J Refract Met Hard Mater 2012;31:258-62.